Chiral Anion in Asymmetric Catalysis

2010. 1. 30 Ryo Yazaki

Review Lacour, J. *et al. Chem. Soc. Rev.* **2003**, *32*, 373.
Chem. Commun. **2009**, 7073.
Macchioni, A. *Chem. Rev.* **2005**, *105*, 2039.

■ Several interactions in asymmetric catalysis

1) Lewis acid chemistry

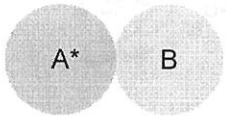

(Lewis acid + Lewis base)

2) Phase-transfer catalysis

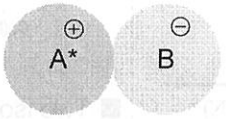

cf) Cinchona alkaloid
Maruoka catalyst

3) Chiral anion

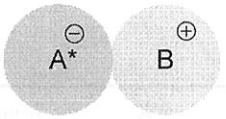

This literature seminar

Maruoka, K. *et al. Chem. Rev.* **2003**, *103*, 3013.
2007, *107*, 5656.

■ Concept of the ion pairs (contact ion pairs): Bjerrum, N. *Sven. Kem. Tidskr.*, **1926**, *38*, 2.

An ion pair is defined to exist when a cation and an anion are close enough in space with a common solvation shell, the energy associated with their electrostatic attraction being larger than the thermal energy (RT) available to separate them. The ions need also to stay associated longer than the time required forBrownian motion to separate non-interacting species

■ Ion pairs in solvent

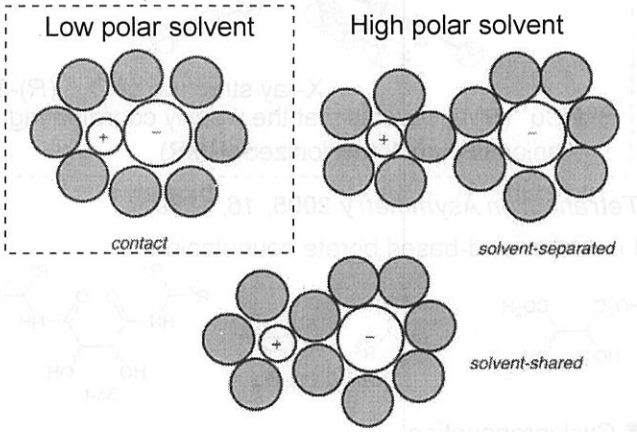

■ Counteranion vs Brønsted acid

"strict" electrostatic *ion pair*

H-bonded charge-assisted supramolecular entity

Brønsted acid catalysis
Akiyama, T. *Chem. Rev.* **2007**, *107*, 5744.
Terada, M. *Chem. Commun* **2008**, 4079.

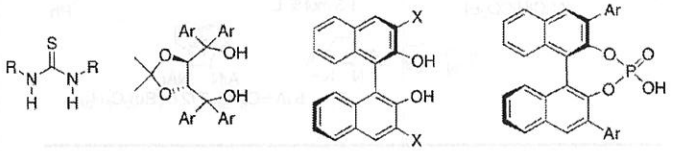

Hydrogen-Bonding Catalysts ⟷ Stronger Brønsted Acid Catalysts

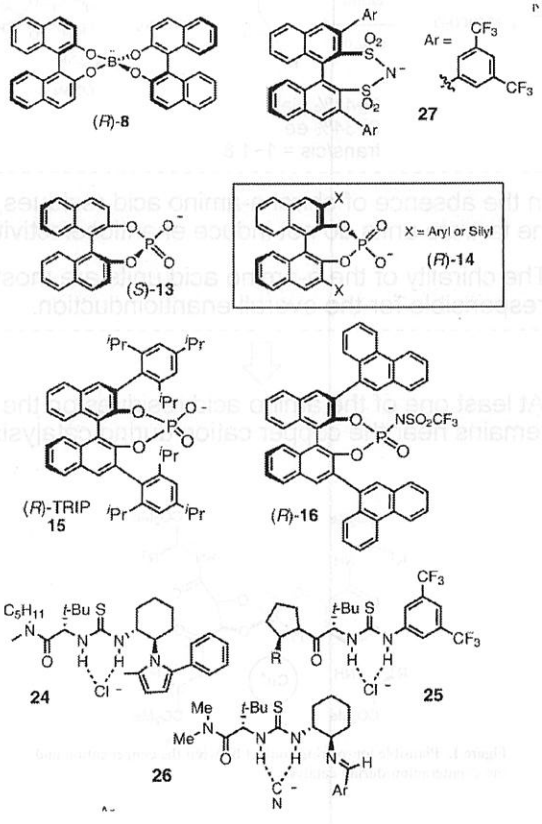

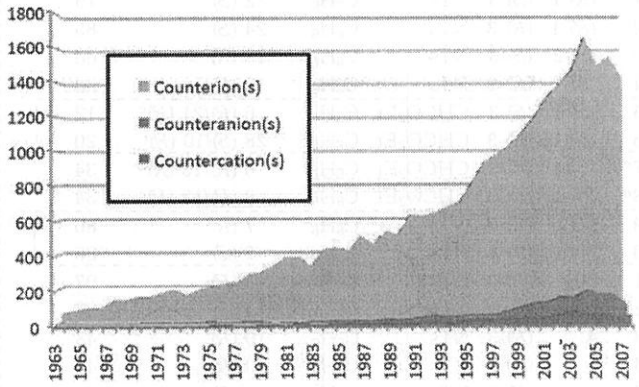

Fig. 28 Number of publications mentioning the terms *counterion* (green), *counteranion* (red) and *countercation* (blue) per year from 1963 to 2008 (singular or plural).

Contents

Arndtsen, B. A. *et al. Org. Lett.*, **2000**, *2*, 4165.

Table 1. Counteranion Influence on CuX-Catalyzed Styrene Aziridination[a]

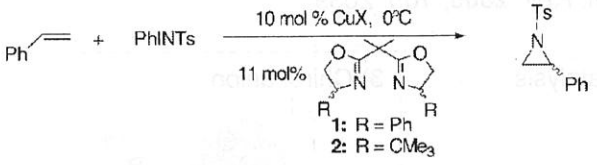

ligand	X	% ee (C_6H_6)[b]	% ee (MeCN)[b]
(*R*)-**1**	OTf	1 (*S*)	28 (*S*)
(*R*)-**1**	ClO_4	5 (*S*)	28 (*S*)
(*R*)-**1**	Cl	17 (*S*)	28 (*S*)
(*R*)-**1**	PF_6	33 (*S*)	28 (*S*)
(*S*)-**2**	OTf	66 (*R*)	2 (*R*)
(*S*)-**2**	ClO_4	57 (*R*)	2 (*R*)
(*S*)-**2**	Cl	26 (*R*)	2 (*R*)
(*S*)-**2**	PF_6	33 (*R*)	2 (*R*)

[a] [styrene]/[PhINTs] = 5. [b] Major enantiomer in parentheses, determined by HPLC on a (*S,S*) Whelk-O 1 column (Regis).[11c]

- This anion influence on enantioselectivity (no consistent trend with either the coordinating ability or size of the anion)
- The ee's are independent of X- in the more polar acetonitrile solvent.

⟶ chiral counteranion strategy is reasonable?

Scheme 1

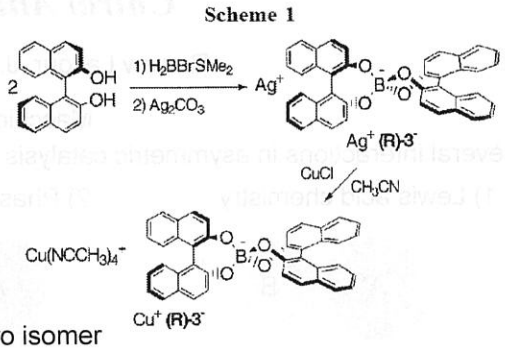

- Two isomer
  1) 1:1 ratio: the tetrakis(acetonitrile) copper-(I) salt
  2) (R)-**3**-, is coordinated through an oxygen atom to a $Cu(NCMe)_3^+$fragment

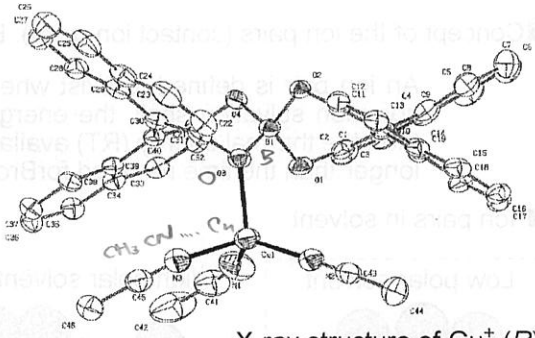

X-ray structure of Cu^+ (*R*)-**3**-

- Cu^+ (*R*)-**3**- reveals that the weakly coordinating anion is completely ionized (NMR)

Tetrahedron Asymmetry **2005**, *16*, 1789.

- α-Amino acid-based borate counetanion

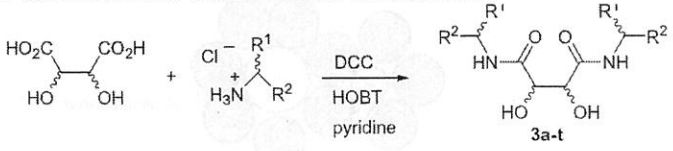

- Cyclopropanation

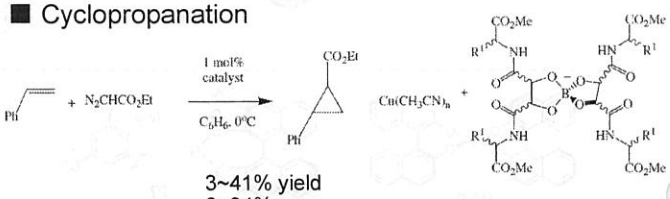

3~41% yield
0~34% ee
trans/cis = 1~1.8

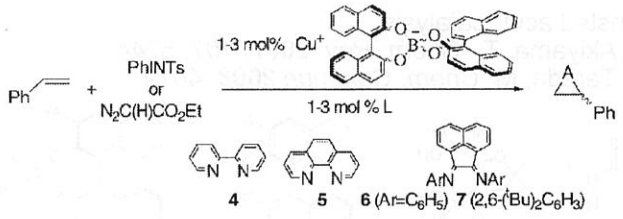

entry	L	X	A	solvent	% ee[b]	yield, %
1	(*R*)-**1**	(*S*)-**3**	NTs	C_6H_6	22 (*S*)	75
2	(*R*)-**1**	(*R*)-**3**	NTs	C_6H_6	24 (*S*)	85
3	(*S*)-**2**	(*S*)-**3**	NTs	C_6H_6	13 (*R*)	nd
4	(*S*)-**2**	(*R*)-**3**	NTs	C_6H_6	12 (*R*)	nd
5	(*S*)-**1**	(*S*)-**3**	$CHCO_2Et$	C_6H_6	6 (*R*)/21 (*R*)[c]	12
6	(*S*)-**1**	(*R*)-**3**	$CHCO_2Et$	C_6H_6	28 (*S*)/10 (*R*)[c]	20
7[d]	(*S*)-**1**	(*S*)-**3**	$CHCO_2Et$	C_6H_6	6 (*R*)/15 (*R*)[c]	34
8[d]	(*S*)-**1**	(*R*)-**3**	$CHCO_2Et$	C_6H_6	8 (*R*)/12 (*R*)[c]	34
9	none	(*R*)-**3**	NTs	C_6H_6	7 (*R*)	86
10	none	(*S*)-**3**	NTs	C_6H_6	7 (*S*)	88
11	none	(*R*)-**3**	NTs	CH_2Cl_2	4 (*R*)	97
12	none	(*R*)-**3**	NTs	CH_3CN	<1	87
13	**4**	(*R*)-**3**	NTs	C_6H_6	10 (*R*)	43
14	**5**	(*R*)-**3**	NTs	C_6H_6	10 (*R*)	41
15	**6**	(*R*)-**3**	NTs	C_6H_6	2 (*R*)	90
16	**7**	(*R*)-**3**	NTs	C_6H_6	<1	78

[a] [styrene]/[PhINTs] = 5 at 0 °C. Aziridination: 3 mol % of Cu^+3^-, 3.1 mol % of L, analyzed by HPLC on an (*S,S*) Whelk-O 1 column (Regis). Cyclopropanation: 1 mol % of Cu^+ 3^-, 1.1 mol % of L, analyzed by GC on a CP Chirasil-Dex column.[12b] [b] Major enantiomer at C1 in parentheses. [c] ee(*cis*)/ee(*trans*). [d] 25 °C.

- The chirality of the counteranion can indeed influence the asymmetric environment about the metal-ligand complex. (entries 5 and 6)
- The first example of an enantioselective transition metal catalyzed reaction where the sole source of chirality is the counteranion (entries 9 and 10)

- In the absence of chiral a-amino acid residues, the tartrate units do not induce enantioselectivity
- The chirality of the a-amino acid units are mostly responsible for the overall enantioinduction.

⇩

- At least one of the amino acid residues on the anion remains near the copper cation during catalysis

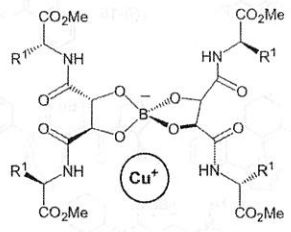

Figure 1. Plausible ion-pairing contact between the copper cation and the counteranion during catalysis.

Nelson, A. *et al. Tetrahrdron Asymmetry*, **2003**, *14*, 1995.

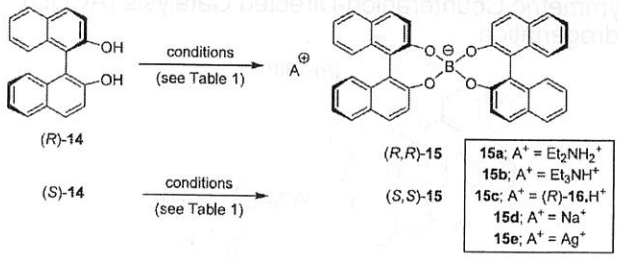

Table 1. Preparation of salts **15** with the chiral counterion **7**

Entry	Starting material	Conditions	Amine	Product	$[\alpha]_D^{20}$ (*c* in DMSO)	Yield (%)
1a	(*R*)-**14**	A	Et_2NH	(*R,R*)-**15a**	−265 (1.10)	88
1b	(*S*)-**14**	A	Et_2NH	(*S,S*)-**15a**	+271 (1.09)	84
2a	(*R*)-**14**	A	Et_3N	(*R,R*)-**15b**	−232 (1.01)	82
2b	(*S*)-**14**	A	Et_3N	(*S,S*)-**15b**	+249 (0.92)	85
3a	(*R*)-**14**	A	(*R*)-**16**	(*R,R*)-**15c**	−239 (1.06)	31
3b	(*S*)-**14**	A	(*R*)-**16**	(*S,S*)-**15c**	+321 (1.05)	37
4	(*R*)-**14**	B	–	(*R,R*)-**15d**	+174 (1.04)	42
5	(*R*)-**14**	C	–	(*R,R*)-**15e**	+136 (1.05)	15

A: $B(OH)_3$, amine, MeCN, Δ, 12 h; B: $Na_2B_4O_7{\cdot}10H_2O$, NaOH, $THF{-}H_2O$; C: 1. $BH_2Br{\cdot}Me_2S$, CH_2Cl_2; 2. Ag_2CO_3, MeCN.

■ Reaction of N-methyl indol with iminium ion

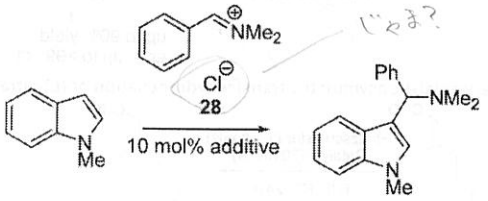

up to 11% ee

■ Ring-opening of an aziridinium ion

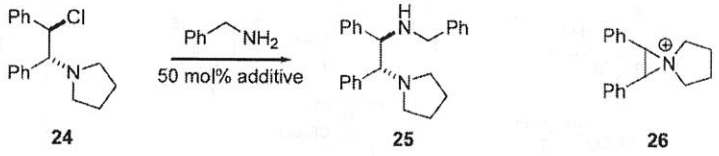

up to 15% ee

Toste, F. D. *J. Am. Chem. Soc.* ***2008***, 130, *14984*

■ Chiral anions could provide a much-needed solution to the problem of reactions proceeding through cationic intermediates that do not possess a (Lewis or Brønsted) basic site capable of coordinating to a metal or proton.

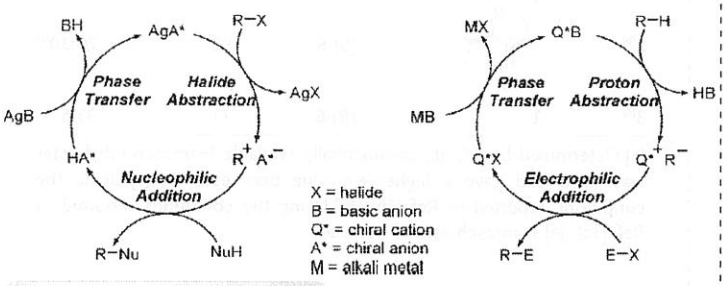

Chiral anion phase transfer catalysis *Chiral canion phase transfer catalysis*

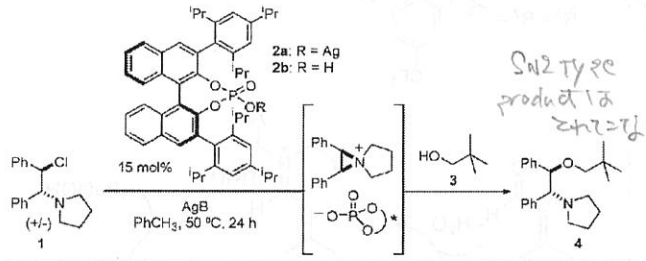

entry	catalyst	AgB	additive	yield (%)[a]	ee (%)[b]
1	**2a**	Ag_2CO_3	none	77	94
2	**2a**	AgOTs	none	88	56
3	**2b**	Ag_2CO_3	none	74	94
4	**2b**	none	none	trace	ND
5	none	Ag_2CO_3	none	trace	ND
6	**2b**	Ag_2CO_3	4Å ms	84	94
7	**2b** (recycled)	Ag_2CO_3	4Å ms	83	94

[a] Conditions: 15 mol % **2**, 1.2 equiv (in Ag) AgB, 4 equiv **3**, 0.1 M in toluene, 50 °C, 24 h. Yields refer to isolated material. [b] Determined

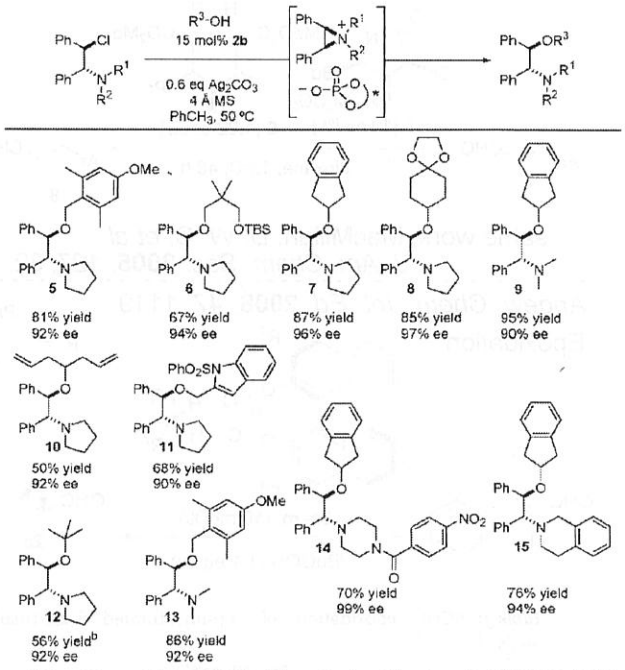

[a] Conditions: 15 mol % **2b**, 0.6 equiv Ag_2CO_3, 4 equiv R^3OH, 0.1 M in toluene, 4Å MS, 50 °C, 24–36 h. Yields refer to isolated material; ee's

■ Asymmetric Opening of Episulfonium Ions

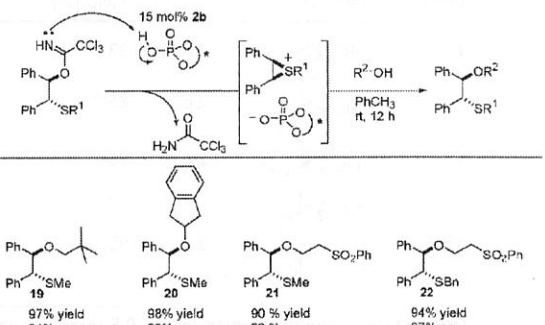

[a] Conditions: 15 mol % **2b**, 2 equiv R^2OH, 0.1 M in toluene, room temp, 12 h. Yields refer to isolated material; ee's determined by chiral HPLC.

■ No example of asymmetric catalysis

■ They could not simply employ silver-halide abstraction method of cation generation, since the sulfide would likely bind Ag^+.

■ Mechanistically distinct from chiral Bronsted catalyzed reactions

List, B. *et al.* . *Angew. Chem., Int. Ed.* **2004**, *43*, 6660.

precedent work

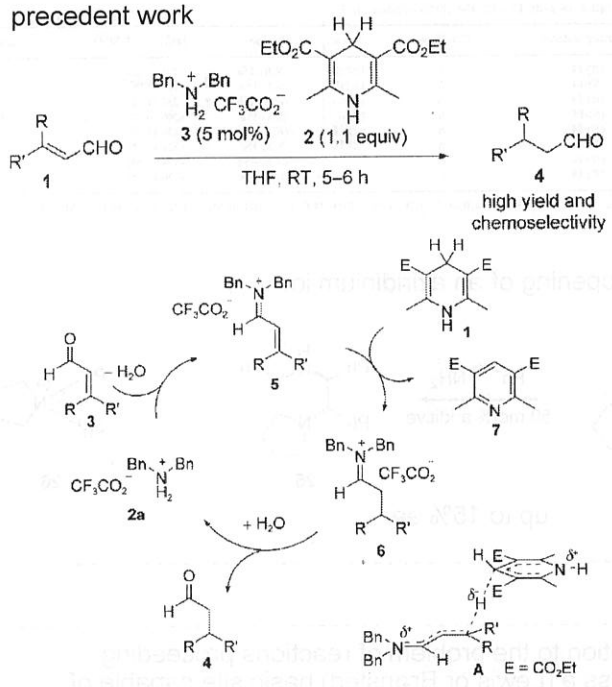

Angew. Chem., Int. Ed. **2005**, *44*, 108.

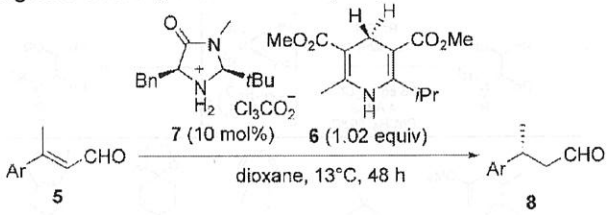

same work; MacMillan, D. W. C. *et al.*
J. Am. Chem. Soc. **2005**, *127*, 32.

Angew. Chem., Int. Ed. **2006**, *45*, 4193

Asymmetric Counteranion-Directed Catalysis (ACDC) Hydrogenation

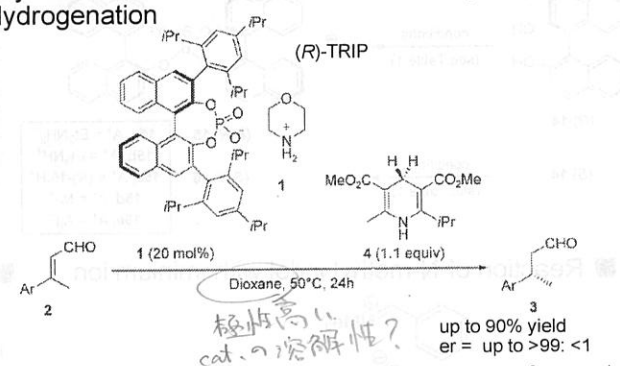

極性高い cat.の溶解性？

Table 2: Organocatalytic asymmetric transfer hydrogenation of (*E*)-citral.

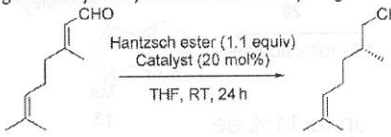

Entry	Catalyst	Product	Yield [%]	e.r.[a]
1[b]	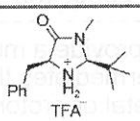	(*S*)-**6**	58[a]	70:30[c]
2[b]	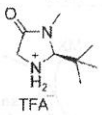	(*S*)-**6**	82[a]	70:30[d]
3[e]	**1**	(*R*)-**6**	71	95:5

[a] Determined by GC. [b] Commercially available Hantzsch ethyl ester was used and gave a higher e.r. value than ester **4**. [c] Using the conditions reported in Ref. [3b]. [d] Using the conditions reported in Ref. [3c]. [e] Hantzsch ester **4** was used.

Angew. Chem., Int. Ed. **2008**, *47*, 1119.

Epoxidation

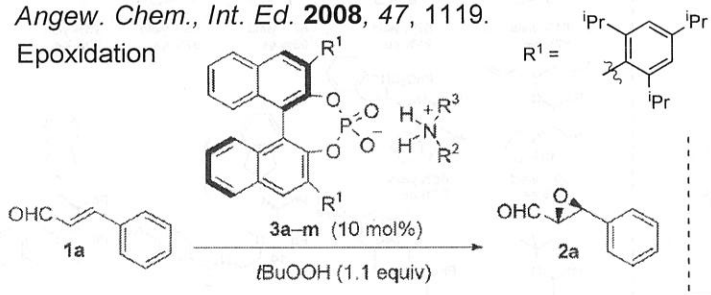

Table 3: ACDC epoxidation of α,β-unsaturated 1,2,2-trisubstituted enals.[a]

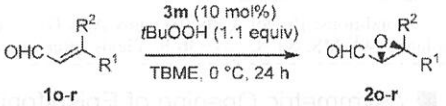

Entry	Product		Yield [%][b]	e.r.[c]
1		**2o**	83	97:3
2	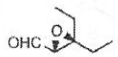	**2p**	85[d]	97:3
3	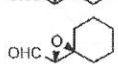	**2q**	75	95:5
4[e]	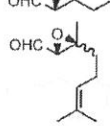	**2r**	95	72:28 d.r. 88:12 e.r. (*trans*) 96:4 e.r. (*cis*)

[a] Reactions were performed on a 0.5-mmol scale with respect to aldehyde in TBME (2 mL) at 0°C for 12 h or 24 h for **1o** and **1p–r**, respectively. [b] Yield of isolated products. [c] Determined by chiral GC. [d] Determined by GC with internal standard. [e] At room temperature.

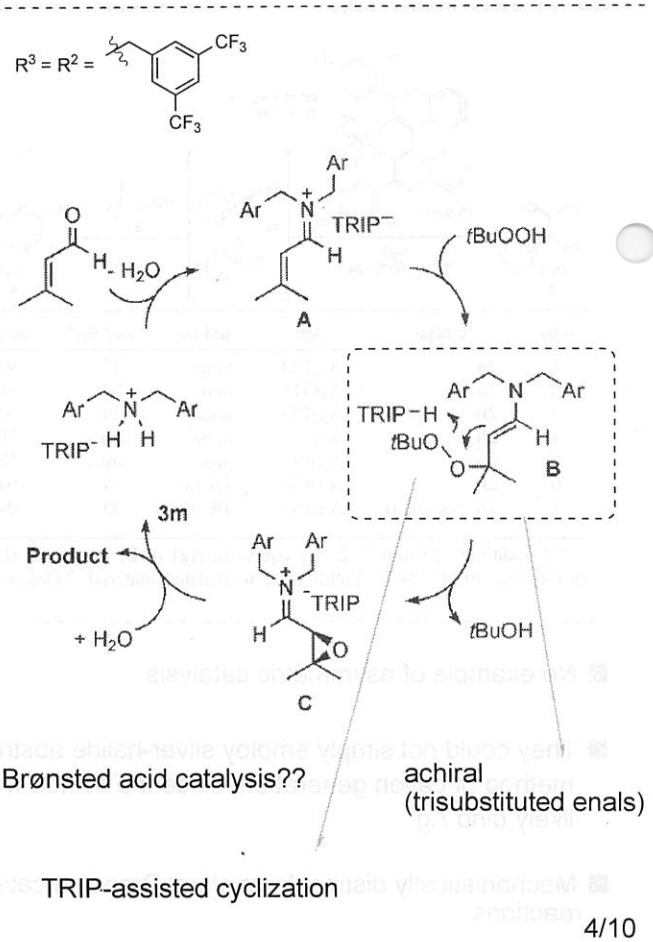

Brønsted acid catalysis??

achiral (trisubstituted enals)

TRIP-assisted cyclization

J. Am. Chem. Soc. **2007**, *129*, 11337. Chiral counteranion in asymmetric transition metal catalysis

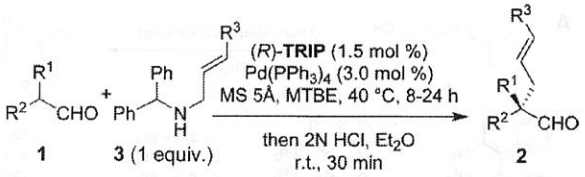

entry	R^1	R^2	R^3		yield (%)	er[a]
1	Me	Ph	H	**2a**	85	98.5:1.5
2	Me	4-Me-C_6H_4	H	**2b**	89	97:3
3	Me	3-Me-C_6H_4	H	**2c**	84	98:2
4	Me	3-F-C_6H_4	H	**2d**	85	98:2
5[b]	Me	2-F-C_6H_4	H	**2e**	74	97:3
6	Me	4-*i*-Bu-C_6H_4	H	**2f**	76	97.5:2.5
7	Me	2-naph	H	**2g**	71	97:3
8	Me	2-thiophenyl	H	**2h**	80	93:7
9			H	**2i**	45	95:5
10[c]	Me	*c*-hex	H	**2j**	65	85:15
11[d,e]	Me	Ph	Me	**2k**	40	96:4
12[d,e]	Me	Ph	Ph	**2l**	82	91:9

[a] From GC or HPLC. [b] Reaction run at 50 °C. [c] Reaction run at 110 °C in toluene. [d] Reaction run at 60 °C. [e] Reaction run for 72 h.

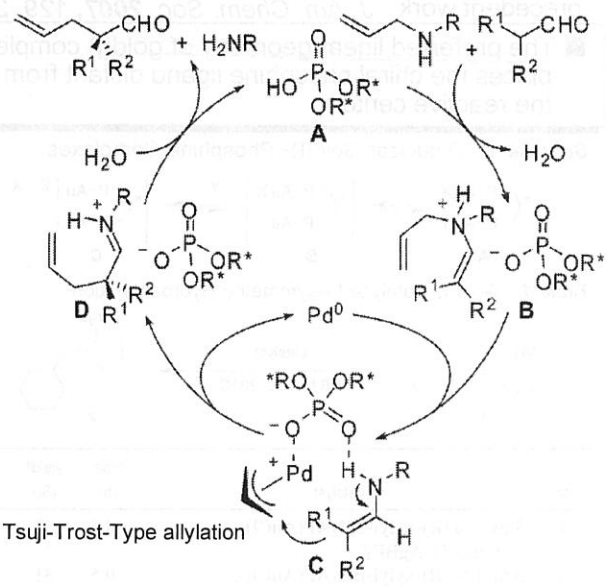

Angew. Chem., Int. Ed. **2009**, *48*, 4363. Mukaiyama aldol

■ up to 0.01mol% catalysis

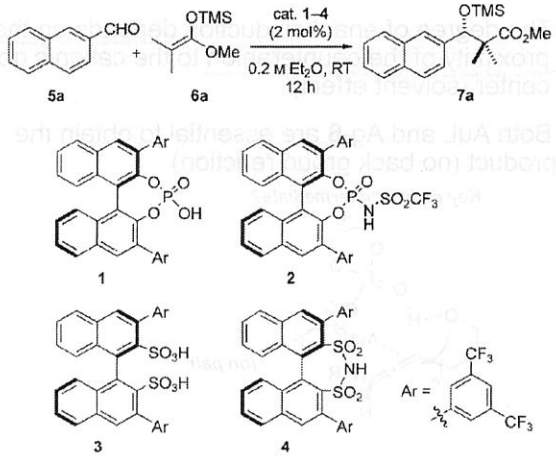

Entry	Catalyst	Yield [%][a]	e.r.[b,c]
1	**1**	<2	–
2	**2**	<2	–
3	**3**	<2	–
4	**4**	>99	90:10

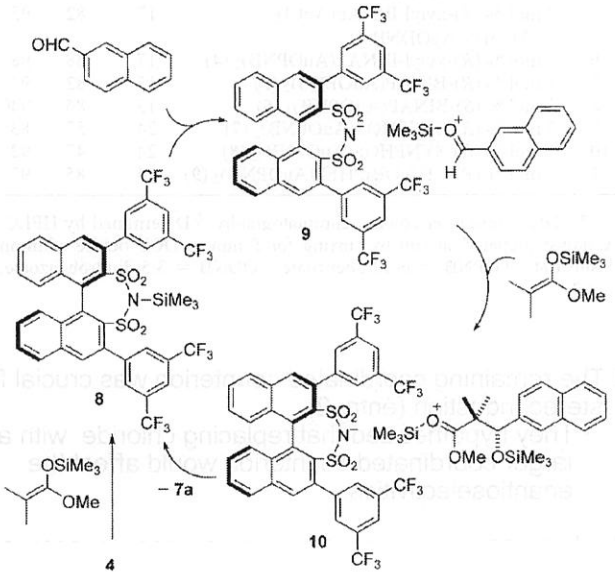

Angew. Chem., Int. Ed. **2010**, *49*, 628, Transition metal catalyzed epoxidation

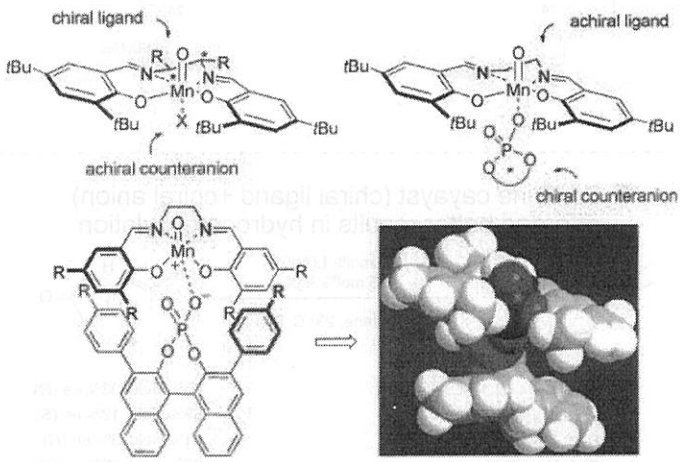

Figure 1. Design principle and modeling of a chiral ion-pair epoxidation catalyst (R = CH_3 in 3D model).

■ Cationic Mn.salen complexes are C2-symmetrical and inherently chiral.even when the salen ligand itself is achiral

■ In case of the Jacobsen.Kastuki epoxidation, the chiral backbone of the salen ligand fixes the complex in one of the two enantiomorphic confirmations

⇩

■ Chiral counteranion should also be able to induce a preference for one of the two enantiomorphic conformations.

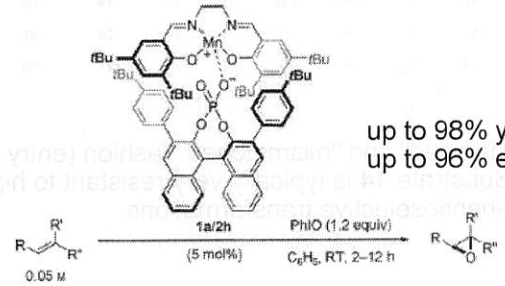

up to 98% yield
up to 96% ee

Toste, F. D. *et al.*

precedent work *J. Am. Chem. Soc.* **2007,** 129, 2452.

■ The preferred linear geometry of gold(I) complexes places the chiral phosphine ligand distant from the reactive center.

Scheme 1. Dinuclear Gold(I)–Phosphine Complexes

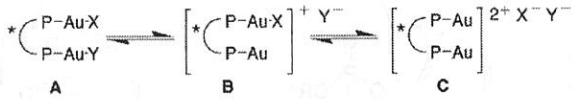

Table 1. Gold(I)-Catalyzed Asymmetric Hydroamination

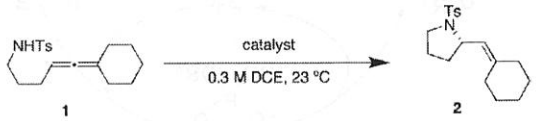

entry	catalyst	time (h)	yield[a] (%)	ee[b] (%)
1	3 mol % (*R*)-xylyl-BINAP(AuCl)$_2$; 6 mol % AgBF$_4$[c]	0.5	82	1
2	3 mol % (*R*)-xylyl-BINAP(AuCl)$_2$; 3 mol % AgBF$_4$[c]	0.5	81	51
3	3 mol % (*R*)-xylyl-BINAP(AuCl)$_2$; 6 mol % AgOBz[c]	24	27	98
4	3 mol % (*R*)-xylyl-BINAP(AuCl)$_2$; 6 mol % AgOPNB[c,d]	24	76	98
5	3 mol % (*R*)-xylyl-BINAP(AuCl)$_2$; 6 mol % AgODNB[c]	17	82	95
6	3 mol % (*R*)-xylyl-BINAP(AuOPNB)$_2$ (**4**)	17	88	98
7	3 mol % (*R*)-BINAP(AuOPNB)$_2$ (**5**)	15	82	93
8	3 mol % (*S*)-BINAP(AuOPNB)$_2$ (**6**)	15	86	94[f]
9	3 mol % (*R*)-SEGPHOS(AuOPNB)$_2$ (**7**)	24	57	83
10	3 mol % (*R*)-SYNPHOS(AuOPNB)$_2$ (**8**)	24	47	92
11	3 mol % (*R*)-ClMeOBiPHEP(AuOPNB)$_2$ (**9**)	15	85	97

[a] Isolated yield after column chromatography. [b] Determined by HPLC. [c] Catalyst prepared in situ by stirring for 5 min in DCE before addition to substrate. [d] OPNB = *p*-nitrobenzoate. [e] ODNB = 3,5-dinitrobenzoate. [f] *ent*-**2**.

■ The remaining coordinated counterion was crucial for stereo induction (entry 2).
→ They hypothesized that replacing chloride with a larger coordinated counterion would affect the enantioselectivities.

Sicence. **2007,** 317, 496.

A

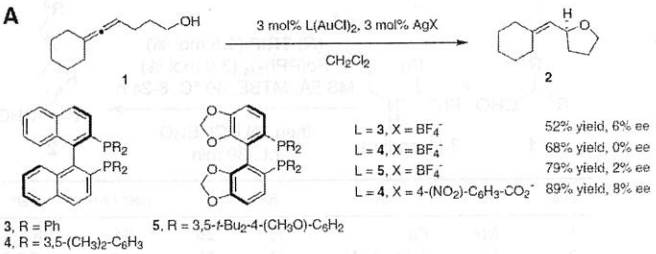

3, R = Ph
4, R = 3,5-(CH$_3$)$_2$-C$_6$H$_3$
5, R = 3,5-*t*-Bu$_2$-4-(CH$_3$O)-C$_6$H$_2$

B

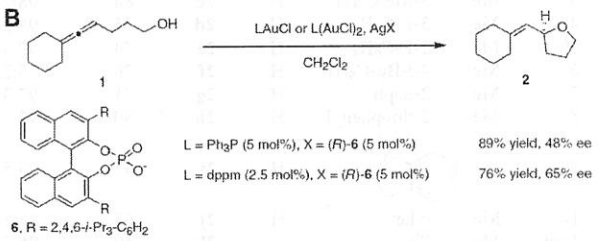

6, R = 2,4,6-*i*-Pr$_3$-C$_6$H$_2$

C

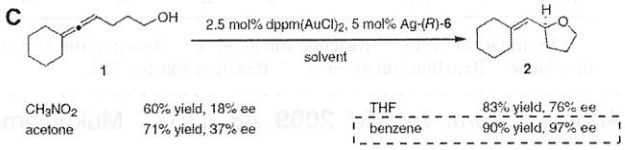

■ The degree of enantioinduction depends on the proximity of the counteranion to the cationic gold center (solvent effect)

■ Both AuL and Ag-**6** are essential to obtain the product (no back groud reaction)

Key cationic intermediate?

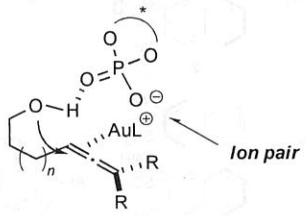

■ Applicable to Hydroamination

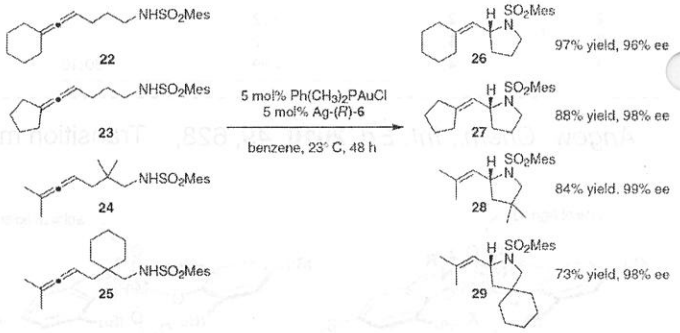

Table 1. Scope of asymmetric hydroalkoxylation. Entry 8 was performed using (*S,S*)-DIPAMP ligand (**7**); enantiomeric excess from using dppm(AuCl)$_2$ is in parentheses. Yields refer to isolated material except for entry 8, which was determined by gas chromatography analysis versus an internal standard.

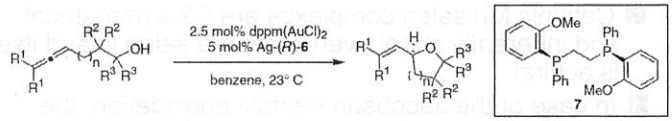

Entry	Substrate	n	R^1	R^2	R^3	Time (h)	Product	% Yield	% ee
1	**1**	1	-(CH$_2$)$_4$-	H	H	1	**2**	90	97
2	**8**	1	CH$_3$	H	H	1	**15**	91	95
3	**9**	1	CH$_2$CH$_3$	H	H	5	**16**	89	96
4	**10**	1	-(CH$_2$)$_4$-	H	CH$_3$	2	**17**	79	99
5	**11**	1	-(CH$_2$)$_4$-	H	Ph	30	**18**	86	92
6	**12**	1	-(CH$_2$)$_4$-	CH$_3$	H	13	**19**	90	90
7	**13**	2	CH$_3$	H	H	15	**20**	81	90
8	**14**	2	H	H	H	24	**21**	96	92 (80)

むずかしい基質

■ "matched" and "mismatched" fashion (entry 8)
Substrate **14** is typically very resistant to highly enantioselective transformations

■ Combine cayayst (chiral ligand +chiral anion) afforded better results in hydrocarboxylation

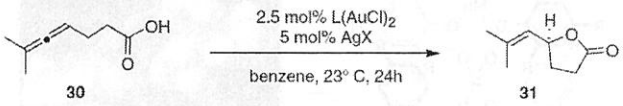

L = (*R*)-**3**, X = 4-(NO$_2$)-C$_6$H$_3$-COO$^-$ 80% yield, 38% ee (*R*)
L = dppm, X = (*R*)-**6** 89% yield, 12% ee (*S*)
L = (*R*)-**3**, X = (*R*)-**6** 91% yield, 3% ee (*R*)
L = (*S*)-**3**, X = (*R*)-**6** 88% yield, 82% ee (*S*)

Further scope; *Angew. Chem., Int. Ed.* **2010,** 49, 598.

Mikami, K. *Angew. Chem., Int. Ed.* **2009,** *48,* 6073.

■ Does the pursuit of atropos ligands always result in efficient asymmetric catalysis?

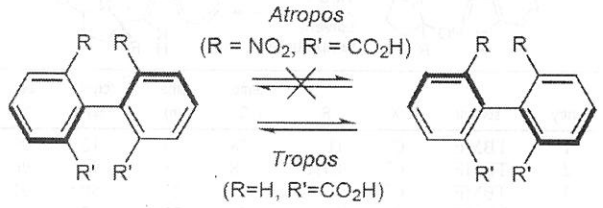

Scheme 1 Atropisomerism of biphenyl compounds

■ Biphep ligand with a torsional barrier of (21~23) kcal/mol would rapidly isomerize at room temperature

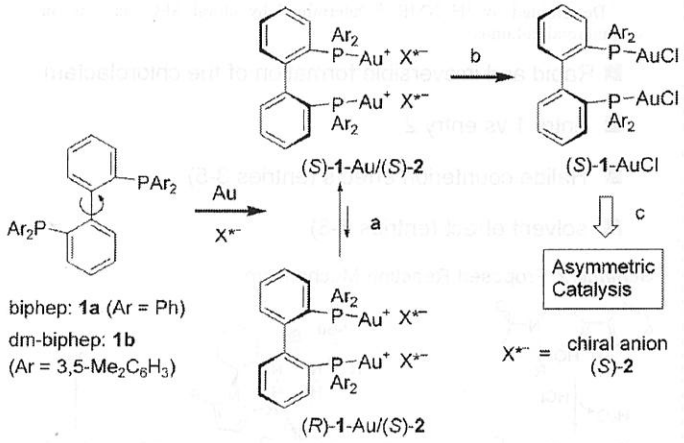

Scheme 1. Strategy of this work. a) Axial chirality control of tropos biphep–gold complexes **1** by using chiral anion **2**. b) Isolation of chirally stable enantiopure biphep–gold complexes below room temperature. c) Application of enantiopure biphep–gold complexes to asymmetric catalysis.

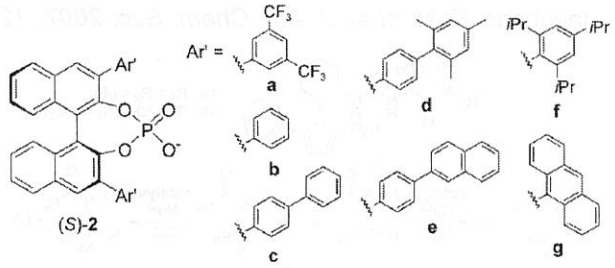

Table 1: Chirality control of biphep–gold complexes using various chiral phosphate anions **2**.[a]

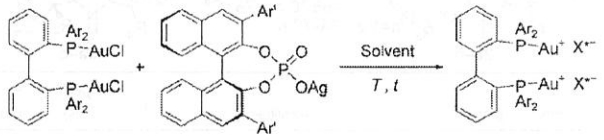

Entry	*rac*-**1**	(*S*)-**2**	Solvent	*T* [°C]	*t* [h]	d.r.[b]
1	**1a**	**2a**	acetone	RT	1	52:48
2	**1a**	**2a**	acetone	80	14	75:25
3	**1a**	**2a**	acetone	100	14	75:25
4	**1a**	**2a**	benzene	100	12	53:47
5	**1a**	**2a**	THF	80	12	71:29
6	**1a**	**2b**	acetone	100	14	96:4
7	**1a**	**2c**	acetone	100	14	99:1
8	**1a**	**2d**	acetone	100	14	100:0
9	**1a**	**2e**	acetone	100	14	100:0
10	**1b**	**2a**	acetone	80	14	87:13
11	**1b**	**2b**	acetone	100	12	89:11
12	**1b**	**2c**	acetone	100	12	100:0
13	**1b**	**2d**	acetone	100	6	decomp.
14	**1b**	**2e**	acetone	100	6	100:0

[a] The use of **2f** and **2g** led to decomposition upon heating. [b] The diastereomer ratio of [(*S*)-**1**-Au/(*S*)-**2**]/[(*R*)-**1**-Au/(*S*)-**2**].

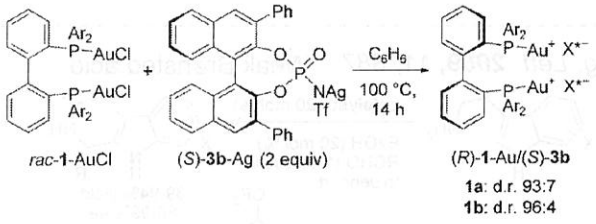

Scheme 2. Chirality control of biphep–gold complexes using chiral *N*-triflyl phosphoramide anion **3b**.

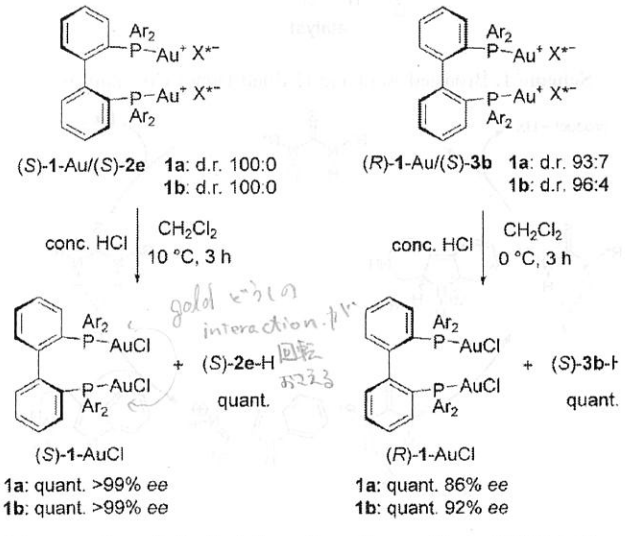

Scheme 3. Quantitative isolation of enantiopure (*S*)- and (*R*)-**1**-AuCl complexes without isomerization and recovery of the chiral anion.

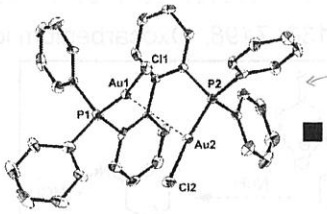

■ Au-Au contact

■ π–π stacking interactions between the two aryl groups on thephosphines

Figure 3. ORTEP view of enantiopure (*S*)-**1a**-AuCl complex showing Au–Au bonding. Ellipsoids are at the 50% probability level; hydrogen atoms and the solvent molecules are omitted for clarity. Selected bond lengths [Å] and angles [°]: Au1–Au2 3.0992(3), Au1–P1 2.2347(18), Au2–P2 2.2383(19), Au1–Cl1 2.2965(18), Au2–Cl2 2.2897(19); P1-Au1-Cl1 169.77(6), P2-Au2-Cl2 173.76(6).

Table 2: Thermodynamic data for the isomerization of enantiopure (*S*)-**1**-AuCl complexes.

Entry	Complex	$t_{1/2}$ [h][c]	$\Delta G^{\ddagger}$ [kcal mol^{-1}][c]	$[\alpha]_D$
1[a]	(*S*)-**1a**-AuCl	406	26.2	+12.8[d]
2[a]	(*S*)-**1b**-AuCl	4097	27.6	+38.6[e]
3[b]	(*S*)-**1b**-AuCl	987	26.8	–

[a] In dichloroethane. [b] In acetone. [c] At 27 °C (300 K). [d] At 25 °C, c = 0.5 in $CHCl_3$. [e] At 27 °C, c = 0.5 in $CHCl_3$.

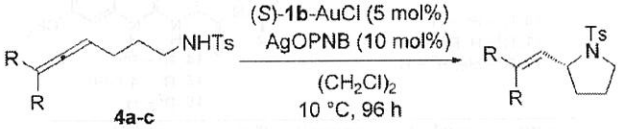

a: R = CH_3
b: R = $-CH_2(CH_2)_2CH_2-$
c: R = $-CH_2(CH_2)_3CH_2-$

5a: 70% yield, 91% *ee*
5b: 61% yield, 75% *ee*
5c: 41% yield, 85% *ee*

Scheme 4. Enantioselective biphep–gold catalyzed intramolecular hydroamination.

Jacobsen, E. N. *et al. J. Am. Chem. Soc.* **2007,** *129,* 2452. Pictet-Spengler-Type

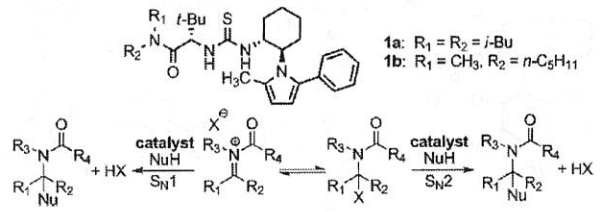

Table 1. Asymmetric Cyclization of Hydroxylactams Catalyzed by **1b**

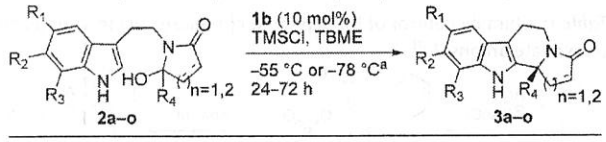

entry	product	substituents	yield[b] (%)	ee[c] (%)
		$n = 1$		
1	**3a**	$R_1 = R_2 = R_3 = R_4 = H$	90	97
2	**3b**	$R_1 = OCH_3$, $R_2 = R_3 = R_4 = H$	86	95
3	**3c**	$R_1 = H$, $R_2 = OCH_3$, $R_3 = R_4 = H$	51	90
4	**3d**	$R_1 = Br$, $R_2 = R_3 = R_4 = H$	88	96
5	**3e**	$R_1 = F$, $R_2 = R_3 = R_4 = H$	89	99
6	**3f**	$R_1 = H$, $R_2 = F$, $R_3 = R_4 = H$	94	97
7	**3g**	$R_1 = R_2 = H$, $R_3 = CH_3$, $R_4 = H$	91	93
8	**3h**	$R_1 = R_2 = R_3 = H$, $R_4 = CH_3$	92	96
9	**3i**	$R_1 = R_2 = R_3 = H$, $R_4 = n$-Bu	74	98
10	**3j**	$R_1 = R_2 = R_3 = H$, $R_4 = C_6H_5$	68	85
11	**3k**	$R_1 = OCH_3$, $R_2 = R_3 = H$, $R_4 = CH_3$	84	91
		$n = 2$		
12	**3l**	$R_1 = R_2 = R_3 = R_4 = H$	52	81
13	**3m**	$R_1 = R_2 = R_3 = H$, $R_4 = CH_3$	63	92
14	**3n**	$R_1 = R_2 = R_3 = H$, $R_4 = n$-Bu	65	96
15[d]	**3o**	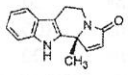	59	88

[a] Unless noted otherwise, reactions of hydroxylactams generated by $NaBH_4$ reduction were carried out at −55 °C, while those generated by alkylation were run at −78 °C. [b] Isolated yield determined after flash chromatography on SiO_2. [c] Determined by chiral SFC analysis on commercial columns. The absolute configuration of **3d** was established by X-ray crystallographic analysis (see Supporting Information). [d] Reaction run for 72 h at −55 °C with 15 mol % of **1b**.

Table 2. Substituent, Counterion, and Solvent Effect Studies

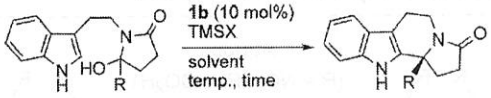

entry	solvent	X	R	temp (°C)	time (h)	conv[a] (%)	ee[b] (%)
1	TBME	Cl	H	−78	8	12	99
2	TBME	Cl	CH_3	−78	8	94	96
3	TBME	Cl	H	−55	23	80	97
4	TBME	Br	H	−55	23	82	68
5	TBME	I	H	−55	23	75	<5
6	TBME	Cl	H	−55	8	65	97
7	THF	Cl	H	−55	8	>95	34
8	CH_2Cl_2	Cl	H	−55	8	>95	<5

[a] Determined by ^1H NMR. [b] Determined by chiral SFC analysis on commercial columns.

- Rapid and irreversible formation of the chlorolactam
- entry 1 vs entry 2
- Halide counterion effects (entries 3-5)
- solvent effect (entries 6-8)

Scheme 2. Proposed Reaction Mechamism

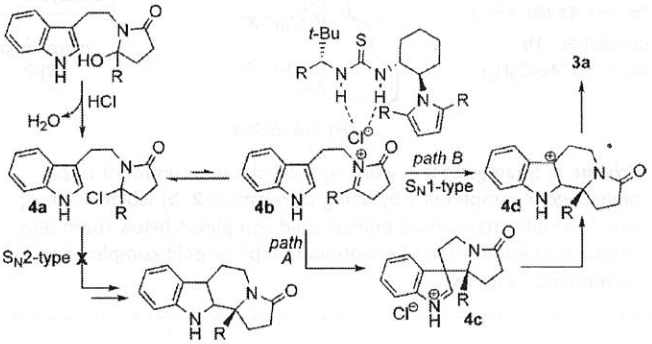

J. Am. Chem. Soc. **2008,** 130, *7198.* Oxocarbenium ions

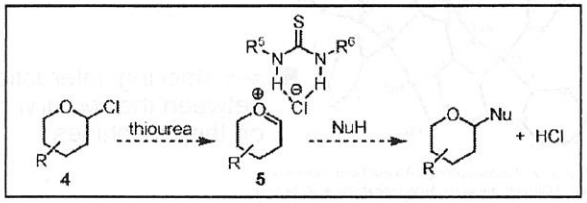

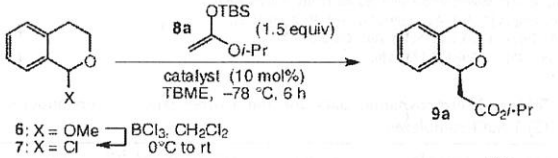

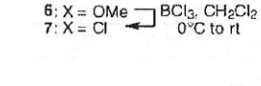

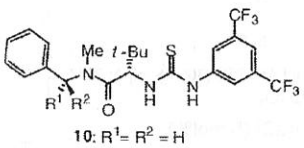

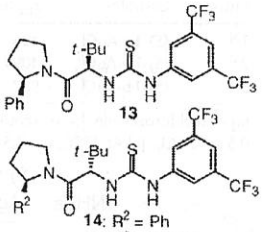

entry	catalyst	conversion (%)[a]	ee (%)[b]
1	**10**	88	63
2	**11**	69	54
3	**12**	97	73
4	**13**	78	−41
5	**14**	96	81
6	**15**	98	85
7	**16**	59	42

Org. Lett. **2009,** 11, *887.* Weak Brønsted acid

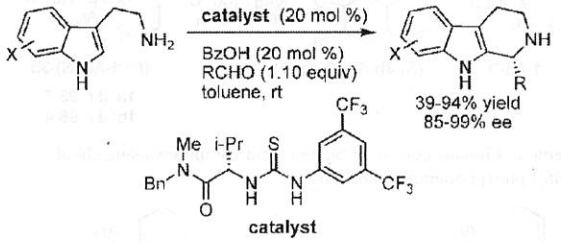

Scheme 1. Brønsted Acid and H-Bond Donor Co-catalysis

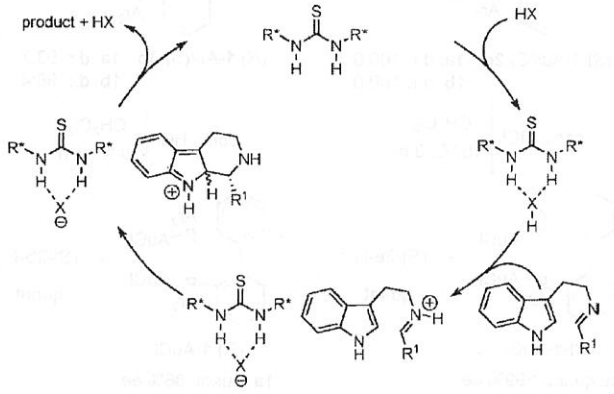

strong achiral Brønsted acid (TfOH?) + chiral thiourea
Science in press

J. Am. Chem. Soc. **2009**, *131*, 15358.

(A) Water-Mediated and (B) Chiral Lewis-Acid Catalyzed

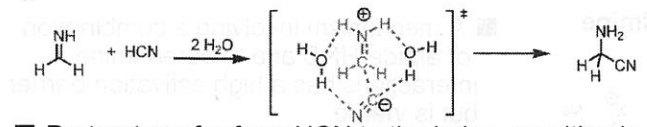

■ Proton transfer from HCN to the imine, resulting in the formation of a reactive iminium/cyanide ion pair

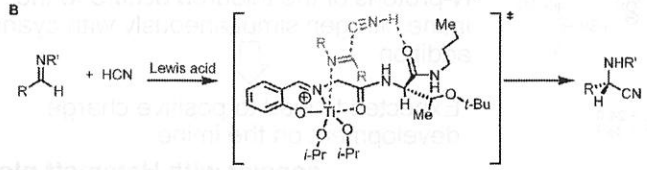

■ Protonation is proposed to occur after nucleophilic addition

Nature. **2009**, *461*, 968.

Scaleable unnatural α-amino acids synthesis

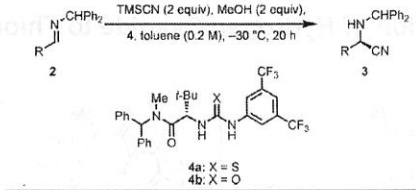

4a: X = S
4b: X = O

entry	cat.	imine 2 (R =)	cat. (mol %)	yield[a] (%)	ee[b] (%)
1	4a	*tert*-butyl (a)	2	99	93
2	4a	*p*-$OMeC_6H_4$ (b)	2	99	99
3	4a	*p*-MeC_6H_4 (c)	2	98	98
4	4a	C_6H_5 (d)	2	98	98
5	4a	*p*-ClC_6H_4 (e)	2	97	98
6	4a	*p*-$CF_3C_6H_4$ (f)	2	98[c]	96
7	4a	*p*-CNC_6H_4 (g)	10	96[c]	93
8	4b	*p*-$OMeC_6H_4$ (b)	2	98	96
9	4b	C_6H_5 (d)	2	97	93
10	4b	*p*-$CF_3C_6H_4$ (f)	2	96[c]	92

■ Kinetic studies

$$\text{rate} = k[\text{HCN}]^a[\text{imine}]^b[\text{cat}]^c_{\text{tot}}$$

$k = 0.58 \pm 0.02\ \text{M}^{-2}\text{s}^{-1}$, $a = 1.09 \pm 0.02$, $b = 1.06 \pm 0.01$, $c = 0.812 \pm 0.007$

deviation from 1st order ↓

(a) No significant catalyst deactivation ("same excess" experiment)
(b) Uncatalyzed background reaction is negligible

Scheme 5. Limiting Mechanisms for Imine Hydrocyanation Proceeding through (A) an Iminium Ion or (B) an α-Amidonitrile Anion

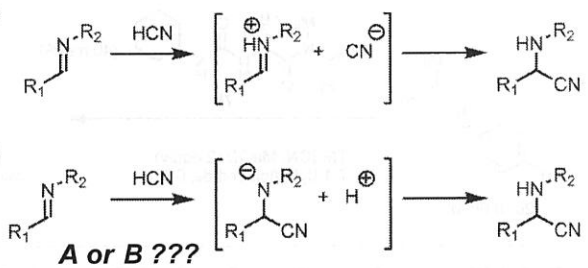

■ Hammett plots

The first-order dependence on both [imine] and [HCN] observed

⟹ The imine reactant is not associated with HCN or catalyst in the resting state

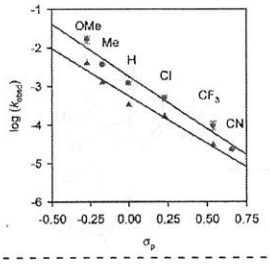

$\rho_{\text{thiourea}} = -2.7 \pm 0.2$; $\rho_{\text{urea}} = -2.5 \pm 0.2$

An increase in positive charge at nitrogen and faster rates are expected with substrates that better stabilize that positive charge

→ Iminium ion mechanism (Scheme 5A)

Catalyst **5** also gave the same results

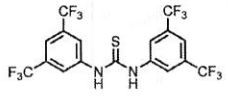

5

■ H-bond donor alone is sufficient for efficient catalysis of this reaction

■ Less electrondeficient anilines leads to a substantial decrease in activity without substantial change in enantioselectivity (entries1-3)

■ Urea-derived catalyst **4b** is slightly less active and enantioselective than **4a** (entries 1 and 4).

■ The amino acid-derived portion of the catalyst affects both activity and enantioselectivity (entries 1, 5-10)

■ The (*R*)-enantiomer is the major product in reactions promoted by (*S*)-amino acid-derived catalysts in all but one case (entry 8).

■ Catalyst **4a** is both the most enantioselective and the most reactive catalyst identified in this series

⟹ Not only destabilization of TS leading to (*S*)-enantiomer but also stabilization of TS leading to (*R*)-enantiomer??

Entry	Catalyst		k_{rel}[a]	er[b]	$\Delta\Delta G^{\ddagger}$ (kcal/mol)[c]
1	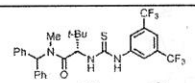	**(4a)**	1.0	47 ± 7	1.86 ± 0.07
2	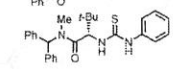	**(6a)**	0.10	32 ± 6	1.67 ± 0.09
3	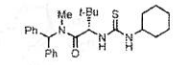	**(7a)**	0.15	49 ± 2	1.88 ± 0.02
4	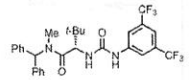	**(4b)**	0.65	23.9 ± 0.4	1.53 ± 0.01
5	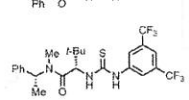	**(4c)**	0.32	12.8 ± 0.2	1.23 ± 0.01
6	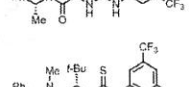	**(4d)**	0.27	5.5 ± 0.1	0.82 ± 0.01
7	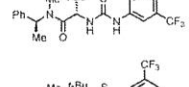	**(4e)**	0.17	1.80 ± 0.01	0.285 ± 0.002
8	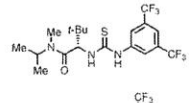	**(4f)**	0.16	0.84 ± 0.01	−0.084 ± 0.008
9	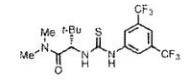	**(4g)**	0.42	6.00 ± 0.04	0.865 ± 0.003
10	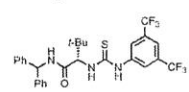	**(4h)**	0.04	1.78 ± 0.07	0.28 ± 0.02

■ Computational analysis

1. Addition of Hydrogen Cyanide to Thiourea-Bound Imine

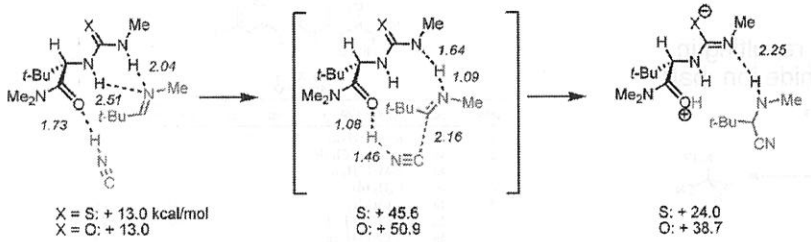

■ A mechanism involving a combination of amide-HNC and thiourea-imine interactions has a high activation barrier but is **viable**

■ Proton transfer from one of the N-protons of the thiourea occurs to the imine nitrogen simultaneously with cyanide addition

⇩

Expected to lead to positive charge development on the imine

consist with Hammett plot

However rule out because.....

■ Thiourea **4a** catalyzes imine hydrocyanation of a range of substrates only slightly more rapidly than urea **4b**

■ Deutrium experiment

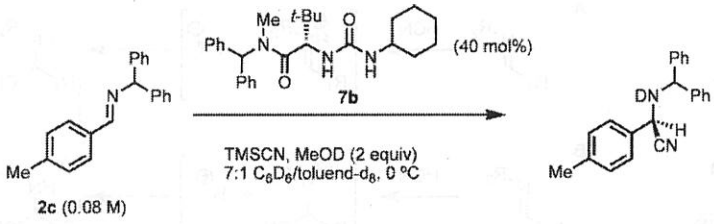

Hydrocyanation of imine **2c** proceeds more rapidly than hydrogen/deuterium exchange between DCN and N-proton of **3b**

---

2. Addition of Cyanide to Catalyst-Bound Iminium Ion.

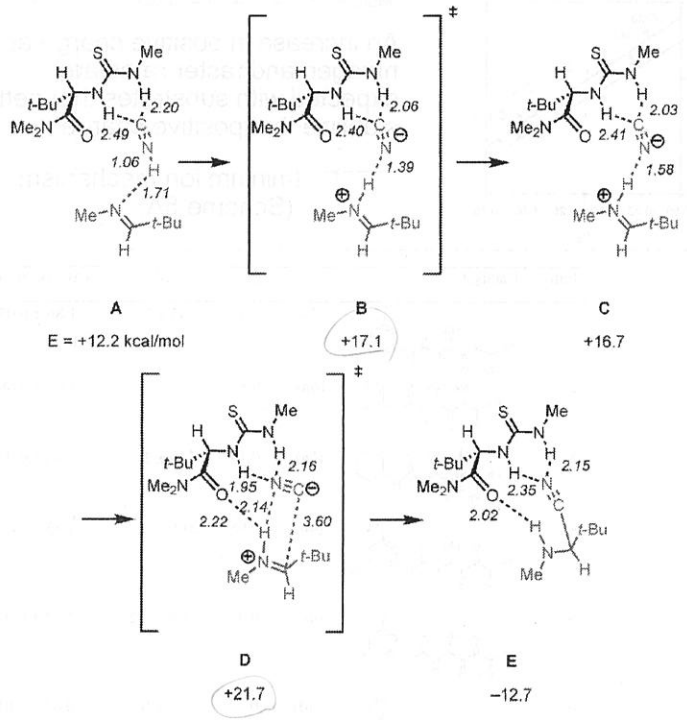

■ Proton transfer from HNC to imine to generate a catalyst-bound iminium/cyanide ion pair

■ The overall activation barrier for HNC addition is slightly lower than for HCN addition

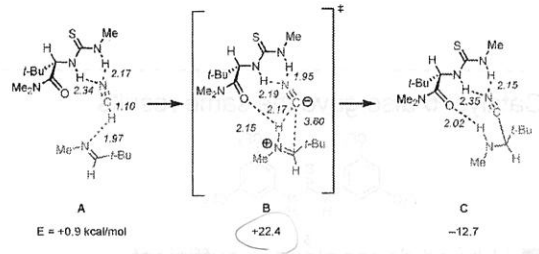

■ Consistent with the Hammett analysis

■ Consistent with the experimental observation that α-aminonitrile N-proton originates from the nucleophile rather than from the catalyst

■ 20 kcal/mol lower than hydrocyanation by direct addition to a catalyst-bound imine.